The Impact of Physicochemical Modification On Iron Oxide Nanoparticle Relaxation Enhancement in Biomedical Imaging in The Anticancer Sector

Homeira Faridnejad*

Ph.D. Candidate in Department of Physics, East Carolina University, Howell Science Complex, Greenville, NC 27858, United States

Corresponding Author: *Homeira Faridnejad, Ph.D. Candidate in Department of Physics, East Carolina University, Howell Science Complex, Greenville, NC 27858, United States*

E-mail: Faridnejadh21@students.ecu.edu

ABSTRACT

The usage of iron oxide nanoparticles for medical applications is also common. The FDA has given Ferumoxytol permission to treat anemia in CKD patients. Due to their tiny size and built-in imaging capability, iron oxide nanoparticles are excellent candidates for Theranostics applications. In this regard, several preliminary clinical proof-of-concept investigations have already been carried out. Among them is the application of ferumoxytol as an additional diagnostic tool in tumor-specific Nano therapeutic settings. Numerous Theranostics iron oxide-based nanoparticles have been created and put through testing for use in drug delivery, particularly for cancer, and are frequently paired with magnetic drug targeting or magnetic fluid hyperthermia. Microbubbles containing iron oxide nanoparticles can assist in gathering important data on the efficacy of sonoporation, which has the potential to improve medicine delivery to malignancies and the brain. Iron oxide nanoparticles are also frequently used in Theranostics settings in regenerative medicine. Today, scaffold materials are commonly labeled with iron oxide nanoparticles in addition to stem cell tracking, which is already done in the clinic. This enables longitudinal monitoring of their performance and function as well as visualizing tissue engineering implants before, during, and after implantation. Overall, the use of iron oxide nanoparticles for biomedical purposes appears to have a bright and promising future. The medical image processing and repository strategies that have been discussed in the literature are reviewed in this work as a tutorial.

Keywords: Biomedical imaging, MRI, Nanomedicine, Theranostics, Anticancer sector, Physicochemical.

INTRODUCTION

Creation and use of iron oxide nanoparticles

By altering the relaxation time of the tissues in which they are present, contrast agents like iron oxide, improve MR pictures [1]. Additionally, they can be utilized to mark specific molecular imaging probes [2]. Unfortunately, there are no molecular imaging probes for clinical MRI on the market right now. Nanotechnology, in which Superparamagnetic Iron Oxide Nanoparticles (SPI-ONS) are created for MR contrast enhancement and/or molecular imaging, is a promising platform for the development of MRI contrast materials. There are numerous ways to make SPIONs, and the best method depends on which characteristics are most crucial for a given application [3]. Additionally, SPIONS' use in molecular imaging is influenced by their capacity to bind molecular markers [4].

There are numerous reviews available on SPION synthesis for MRI [5]. Nevertheless, they frequently cater to chemistry stu-

dents [6]. The creation of MRI contrast agents draws seasoned experts from a variety of disciplines, including some who are unfamiliar with MRI or medical imaging [7]. Depending on their level of dedication and aptitude for learning, this role allows radiation doctors the chance to take part, work with others, or organize research. The understanding, expertise, and abilities required to contribute to the advancement of MRI and molecular imaging are now mostly in the hands of medical radiologists [8,9]. Their knowledge of radiation protection, patient care, and imaging technology equips them with abilities that are immediately useful to research into the creation and use of SPION and MRI [10,11].

Multidisciplinary in nature, applied physics, mechanics, chemistry, electrical and biological engineering, machine design, robotics, and medicine have all been transformed by nanotechnology. The creation of nanoparticles in medical imaging has received a lot of studies, particularly for uses in molecular imaging [12,13]. Since these particles are, Nanosized (less than 100 nm); they can bind to a wide variety of molecular markers that can interact with one another at the molecular and cellular levels, opening up a wider spectrum of disease targets for molecular imaging [14].

Additionally, nanoparticles have the power to completely alter current imaging methods. The combination of high sensitivity and great spatial resolution needed for molecular imaging is not present in conventional imaging techniques. High-sensitivity nuclear medicine techniques like Single-Photon Emission Computed Tomography (SPECT) and positron emission tomography offer improved sensitivity at the expense of decreased spatial resolution. MRI has a high resolution but lacks sensitivity to molecular signals [15,16]. Nanoparticles have the potential to significantly improve sensitivity and provide high-resolution molecular imaging during procedures like MRI [17]. High spatial resolution, non-invasive, non-ionizing radiation, and multi-plane tomography capabilities are all features of MRI. MRI can design nanoparticles to include ligands that target particular molecules and have magnetic characteristics that are detectable at low doses [17]. Since iron oxide nanoparticles are primarily superparamagnetic, they have received extensive research attention for MRI. Iron oxide nanoparticles come in a variety of forms, including magnetite (Fe_2O_3), magnetite (Fe_3O_4), and hematite (Fe_2O_3). Magnetite (Fe_3O_4) is particularly promising due to its established biocompatibility [15].

Superparamagnetic Iron Oxide Nanoparticles (SPIONS) should be magnetic, nontoxic, and biocompatible for molecular imaging applications. Additionally, they need to interact with a variety of medications, proteins, enzymes, antibodies, or other molecules. A variety of methods has been used to create SPIONS for use as MRI contrast agents [18]. Particles made with each technique have various sizes and magnetic properties. Additionally, organic material can be used to coat the surface of iron oxide nanoparticles to form an interface between the particles' core and the surrounding medium. The particles can be directed to the desired location using this surface layer.

Magnetic Resonance Imaging (MRI) is a commonly used tool for patient diagnostics because p it is a non-invasive procedure that does not require ionizing radiation and can provide high resolution of anatomical features [19,20]. MRI relies on the use of Contrast Agents (CAs) to enhance image visualization and to further assist in disease characterization and diagnosis. A desirable MRI CA is designed to have high magnetic relaxivity, which influences the positive and negative contrast of an image by changing the relaxation rate of the surrounding hydrogen protons. Among the CAs used widely in MRI are Iron Oxide Nanoparticles (IONPs), which have been well studied and show good biocompatibility, as well as unique biological, chemical, and magnetic properties. This has led to IONPs being extensively used throughout the biomedical field. Unlike gadolinium-based CAs, which have recently been associated with allergic reactions and long-term side effects (such as nephrogenic systemic fibrosis and long-term brain deposition) and discontinued from certain US and European markets, IONPs-based CAs are still being used in clinical diagnosis. More recently, an increasing interest in IONPs-based CAs has resurfaced not only for diagnostic purposes but also for therapy in the clinic.

IONPs are generally crystallized into four different phases: magnetite (Fe_3O_4), hematite (γ-Fe_2O_3), maghemite (α-Fe_2O_3), and quartzite (FeO). The appearance features of Fe_2O_3 exhibit a dark black powder and has colloidal forms (Fe_2O_3 is a dark black powder, and its colloidal forms characterize its appearance) [1]. Once oxidized, it can become maghemite and exhibits a brownish color similar to rust. The unique properties of Fe_3O_4 are due to its size and shape tenability, magnetic ordering, high surface area, and extrinsic response in physiological media. Fe^{2+} cations occupy 25% of the octahedral interstitial sites, while Fe3+ cations occupy 25% of the octahedral sites and 12.5% of the tetrahedral sites. The magnetic moment of iron is too large because it has four unpaired electrons in the 3d orbital, so this magnetic moment can interact with the spin and orbital moment [21]. Fe^{3+} and Fe^{2+} can become ferromagnetic, ferromagnetic, antiferromagnetic, or superparamagnetic since they undergo phase transitions to a magnetically ordered state. Fe_3O_4 with core sizes of 5 nm -20 nm is one of the superparamagnetic nanoparticles which are used as T2 CAs. One of the main challenges is to endow Fe_3O_4 with a high magnetic relaxivity response when they are designed as MRI CAs [21]. MRI produces reflection differences in intensities of resonances of 1H MR Resonances, usually of water protons36. These intensities are proportional to concentrations of 1H and can be modulated by the longitudinal ($R_1=1/T_1$) and transverse ($R_2=1/T_2$) relaxation rates. Therefore, the contrast can be modulated by enhancing the relaxation rates through paramagnetic agents. We can define the properties of magnetic nanoparticles based on their size; however, particle size cannot change the longitudinal relaxation rate r_1 and transverse relaxation rate r_2 of these nanoparticles [22,23]. The relativity of a CA can be thought of as a measure of the sensitivity of the contrast agent, where a higher relaxivity value corresponds to a reduced time constant. There are two types of MRI CAs, one referring to positive CA (T_1) and the other to negative CA (T_2). Fe_3O_4 nanoparticles are commonly used as a T2 CA. This can improve the sensitivity of MRI scans by enhancing the contrast between normal tissue and diseased tissue. The longitudinal (spin-lattice) relaxation time is the time needed to return to equilibrium after being exposed to a magnetic field and is a constant known as T_1. A T_1 CA improves the positive contrast signal being displayed during the MRI scanning [21]. One of the biological parameters of time is transverse (spin-spin) relaxation time which is the time needed to decay or dephase the magnetic moment. In other words, in the MRI system, we have two relaxation times: the spin-lattice (longitudinal relaxation) time T_1 and the spin-spin (transverse) relaxation time T_2. A T_2 CA will improve the negative contrast signal being displayed during the MRI scan (what appears dark) and a T1CA will improve the positive contrast signal and can provide signal enhancement on

T1-weighted images [24]. Both T_1 and T_2 relaxation times have proven to be useful in clinical practice for the differentiation of tissues and assessment of their state. For instance, T_1 in muscle is 900 ms, but T_1 in fat is 30 ms; the main reason for this difference is the size and motion of the molecule in which the hydrogen nucleus resides. T_1-weighted and T_2-weighted images can be created at different times. In MRI, the acceleration of data acquisition is important to do scanning procedures for more patients and to reduce motion artifacts. Usually, MRI T_2-weighted scanning takes more time compared to T_1-weighted scanning due to its longer repetition time and echo time [7,25]. Two sequences of T1-weighted and T_2-weighted images are commonly used for imaging gray matter such as fatty tissue and liver lesions to obtain morphological information. A T_2-weighted image is made by setting a long repetition time and long echo time. This sequence is commonly used for detecting inflammation and edema, revealing white matter lesions, and assessing region-specific anatomy in the prostate or the uterus. More recently, it has been reported that the physicochemical transformation effect of Fe_3O_4 can enhance the T_1 and T_2 relaxivity times. Due to the limitations of MRI images, including their poor physiological information, we can use the CAs with different physicochemical structures to enhance MRI signals [26](Figure 1).
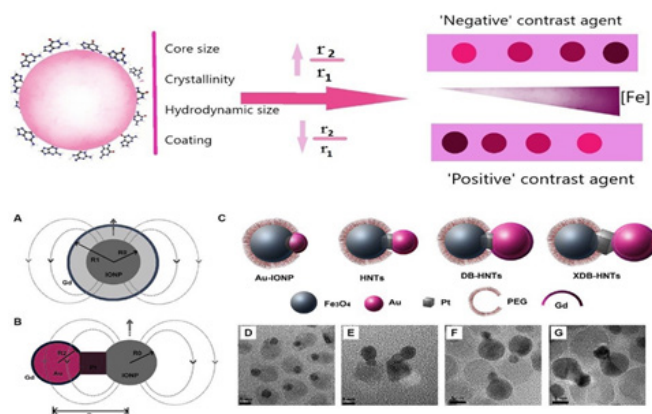

Figure 1. Effects of the different features of using CA such as core size, crystallinity, hydrodynamic size, and coating on MRI

LITERATURE REVIEW

MRI contrast enhancement mechanisms

As mentioned, IONPs react to the presence of a magnetic field, so their superparamagnetic behavior of them remains only shortly in the presence of a magnetic field and these nanoparticles quickly return to their original state as the magnetic field separates [27]. After the synthesis of IONPs, they immediately make an iron oxide layer on their surface. These nanoparticles have a core-shell structure to a pure iron NP and these layers do not penetrate the whole particle [28]. Preparation should be done under anaerobic conditions because Fe_3O_4 NPs are not stable under ambient conditions, and they can be easily dissolved in an acidic medium [29]. Therefore, to prevent it, oxidation should be performed under anaerobic conditions (there is no need to repeat that preparation should be in anaerobic conditions) (Figure 2).
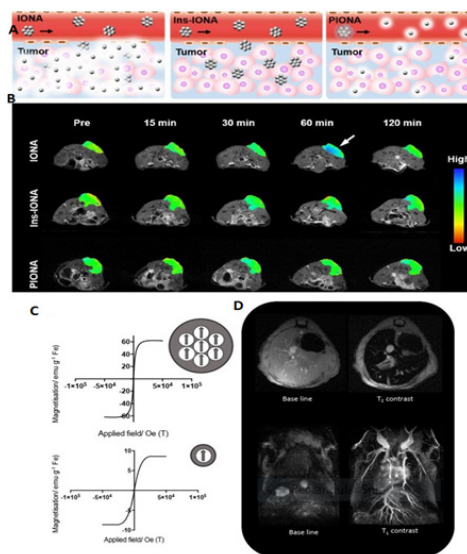

Figure 2. Schematic illustration of the structural changes of iron oxide nanoparticle assemblies
(IONAs), Ins−IONAs, and polymer-assisted IONAs (PIONAs) in blood flow. The IONAs and Ins−IONAs are stable in blood

circulation. After accumulation in the tumor, IONAs further disassemble into dispersed ESIONs for non-linear amplification of MR imaging, while Ins−IONAs remain in the quenched T_1MR state. PIONAs gradually dissociate during blood circulation even before their accumulation in the tumor. T_1-weighted MR images of tumor-bearing mice before and after i.v. injection of IONAs, Ins−IONAs Change in the magnetic behavior of iron oxide nanoparticles with the decrease of the core size, from superparamagnetic to paramagnetic (bottom), Mouse liver T_2-weighted MRI using iron oxide nanoparticles with bigger core size, T_1-weighted MR angiography using iron oxide nanoparticles with smaller core sizes (bottom) [3,10,24,30].

Because oxidation has little effect on Fe_2O_3 nanoparticles in alkaline or acidic conditions, it is essential to preserve the magnetic characteristics of nanoparticles. The highly reactive IONPs of these nanoparticles may result in the loss of their magnetic property [30]. They can employ a variety of defense mechanisms and offer an appropriate surface coating with organic molecules, polymers, biomolecules, and inorganic layers to preserve this property [31]. IONPs also has a built-in mechanism for breakdown, efficient elimination from the body, and metabolism in hemoglobin. Additionally, they have minimal toxicity, a lengthy blood half-life, and just superficial chemical flexibility [32]. By decreasing the Longitudinal Relaxation Time (T_1) and Transverse Relaxation Time (T_2) of water protons, two primary forms of CA are produced in MRI. The goal of a study on novel IONPs for MRI is to achieve transverse relativity values (r_2). Recent studies have employed IONPs as a positive CA with large relaxivity longitudinal values of r.

The interaction of water molecules with a magnetic center is related to the relaxation mechanism by nanoparticles, in which the characteristics of nanoparticles play a crucial role. The Solomon Bloembergen Morgan (SBM) theory and the outer-sphere quantum mechanical theory are two significant ideas that can be utilized to describe the design principles of CA for MRI. Here, we'll give a quick physical explanation of these two theories [25].

Solomon−Bloembergen−Morgan Theory

The SBM theory is an important mechanism related to the T_1 and T_2 relaxation time of water protons and the dipole-dipole interactions proposed in 1948. While bipolar interactions were initially limited to proton-proton interactions, the SBM theory was extended to proton-electron interactions in 1961 [33]. Proton-electron interactions are much stronger than proton-proton interactions because of their small mass and bipolar magnetic moment. This is because an electron's spin is greater than the spin of a proton. Many mathematical equations can be found in this field. This concept simply states that bipolar interaction is inversely related to the distance between the protons to the sixth power (d6) and the direct interaction to the Gyromagnetic Ratio (γ) protons depends on the fourth power ($γ2×γ2$) and the spectral density, which is related to the relationship between Correlation Time (τc) and Larmor frequency [2,34].

Among the motions in molecules, there are three types of vibrational, transient, and rotational motions, but only the rotational motion is considered important in the relaxation of the nuclear magnetic because it occurs within the Larmor frequency of the proton [34].

Unlike proton-proton interactions, proton-electron interactions between water protons, ions, and paramagnetic molecules are central mechanisms alongside paramagnetic materials such as T_1 CA. Water molecules that bind to proteins have a much shorter T_1 relaxation time compared to free water molecules [35]. Because of these conditions, many biological systems can be used. In general, the interactions of water protons with paramagnetic centers are classified by three different mechanisms: inner-sphere, second-sphere, and outer-sphere. Figure 3.
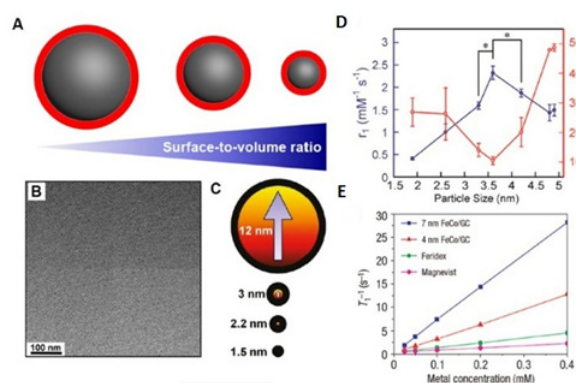

Figure 3. The effect of size on T1 relaxation in MNPs

Figure 3 shows that the size of MNPs depends on the surface-to-volume ratio. The rotating layer is displayed on the surface in red (B and C). Comparison of 12, 2.2, and 1.5 nm SPIONs with TEM images of ultra-small 3 nm SPIONs and rotation models. r1 values and r_2/r_1 ratios of exceedingly small-sized IONPs as a function of the particle size (< 5 nm) [2].

The outer sphere model does not sufficiently define the relaxation profile. The best definition of relaxivity time is when it has both the second sphere and outer-sphere models. Because the contribution of the second-sphere mechanism to relaxation is negligible, it is limited to certain cases where the inner sphere has no coordination with water molecules. Consequently, 10%-30% of the second-sphere mechanism can help relaxivity r_1 [36].

Molecules are generally subjected to three movements: vibration, transfer, and rotation. Transition motion is averaged in a homogeneous field, vibrational motion affects relaxation because of its velocity, and only rotational motion occurs at a range of frequencies that covers the Larmore frequency of protons in nuclear magnetic relaxation. These conditions can be met in many biological systems. For example, T_1 relaxation time is shorter than that of free water molecules in aqueous molecules that bind to proteins or macromolecules. The relaxation time of T_2 relaxation decreases the motion of water molecules as well as the average effect [37].

A key feature that explains why paramagnetic materials are so effective at increasing proton relaxation is that gamma electron spins are more than 360,000 times the difference between electro-proton and proton-proton interactions because γ electron spins are more than 600 times larger than proton spins [38].

CA T_1 Proton-electron interactions between water protons and paramagnetic ions/molecules are the central mechanism of paramagnetic materials. In the classical model, water protons interact with paramagnetic centers and are classified into inner, second, and extraterrestrial mechanisms. In Figure 4 the mechanism of the inner sphere is shown as a chemical exchange, which involves the interaction of bulk water protons and the direct coordination of water protons with paramagnetic ions. Figure.4. The mechanism of the inner sphere is also shown as chemical exchange, which involves the direct coordination of water protons with paramagnetic ions after separation by interaction with bulk water protons [39]. Based on the definition of chemical exchange, the transfer of a nucleus can occur either intra-molecularly or inter-molecularly, describing from one part of a molecule to another. The chemical exchange shortens the relaxation times of T_1 and T_2 depending on the field. The mechanism of the inner sphere is modeled as follows, which dominates the increase of T_1 relaxation in paramagnetic CA.

$$T_{1e} = 1/25\Delta^2\tau_V\left[4S(S+1)-3\right]\left[1/(1+\omega_s^2\tau_v^2)+4/(1+\omega_s^2\tau_v^2)\right] \qquad (1)$$

$$T_{1e} = 1/25\Delta^2\tau_V\left[4S(S+1)-3\right]\left[5/(1+\omega_s^2\tau_v^2)+2/(1+4\omega_s^2\tau_v^2)+3\right] \qquad (2)$$

Where S is the total electron spins of the metal ion, ωS is the angular electronic frequency, and Tie is the electronic relaxation times (i=1,2); Δ is the Zero-Field Splitting (ZFS) energy, and τv is the splitting correlation time.

Surface Modification

To meet the stability criteria, and the ability to target biocompatibility for medical applications, nanoparticles synthesized by thermal methods usually require multi-stage surface modification. Many strategies for nanoparticle surface engineering research have been extensively reviewed in the past decade [40].

Anchoring structure

There are similar strategies for the surface performance of MNPs as for other nanomaterials. Surface ligands are required to stabilize MNPs to prevent particle aggregation, which can be achieved in two ways. Either it is attached to the MNPs through chemical coordination, or physical forces are applied to the MNPs [24]. The anchoring behavior of molecules on MNPs has rarely been studied, but among those studies are the systematic studies of the Pierre group that reported the surface performance of MNPs using anchor sections [20]. The results of this study showed that the magnetic moment could be maintained with nanoparticles coated with PEG polymers, while other parts of the anchor reduce the magnetic field. In general, the nature of anchoring surface molecules in Nano solution is related to T_2 relaxation (Figure 4).
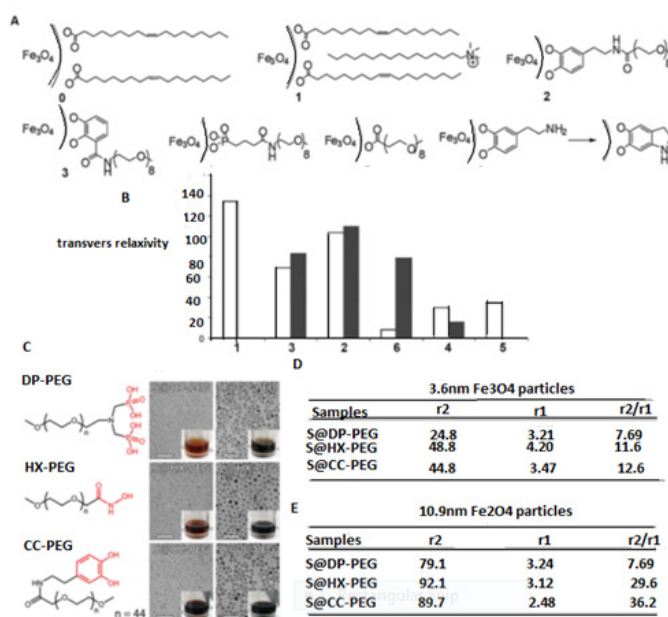

Figure 4. Anchoring structure and the effect on T1 and T2 relaxivities

In Figure 4 Different ligands for surface anchoring of Fe_3O_4 NPs, including oleic acid (0), oleic acid-soap (1), dopamine-PEG (2), DHB-PEG (3), PO3-PEG (4), CO2-PEG (5), and dopamine (6). [2] The M-H curves and transverse relaxivity study of the Fe_3O_4 NPs with different anchoring molecules. (C, D) Chemical structures of PEG with different anchoring groups, TEM images, digital photos, and the r1 and r2 values of Fe_3O_4 nanoparticles (3.6 nm and 10.9 nm in diameter) after surface modification [2].

Assembly

Nanoscience assembly is a phenomenon in which the components of the system come together and form a larger unit through spontaneous interactions or external forces. In nanoscience or chemistry, this phenomenon is described at the scale of molecules or nanoparticles. Nanoparticles are assembled through external iron and surface engineering molecular interactions. Several types of assembly structures have been found with MRI, including T_2 relaxation in unique nanoparticles on MRI. Gillis and Koenig state that a small number of larger particles has a greater effect on relaxation than a large number of smaller particles of the same mass. To achieve mass magnetic properties, the effect of microscopic bonding across crystalline nanoparticles is crucial. However, the basic mechanism of T_2 relaxation on augmented nanoparticle assembly is not yet known [23].

Assembly state

There are two questions about the montage mode: first, what is the fractional ratio of MNPs in the assembled structure, and second, what is the spatial order of the MNPs in the assembled structure. In the first question, montage is created by biological or molecular targets that refer to real systems[128]. With increasing concentration, higher degrees of assembled MNPs with pre-modified functions can be noted (Figure 5). Significantly, the assembly mode is in an optimal range with the T_2 relaxation time of MNPs assembled linearly. The second question arises through artificial or well-defined molecular interactions between MNPs. For example, in Figure, it is expected that through the hydrophobic-hydrophobic interactions with the hydrophobic core during the self-assembly of amphiphilic polymers, the hydrophobic core is achieved. It is based on an automation process that can be controlled as much as possible. The Weller study group presented the relaxation of clusters based on SPIO using limited size. To block SPIOs with a diameter of 9.8 nm, three-block PEI-b-PCL-b-PEG polymers were used, which produced SPA clusters of various sizes from 51 nm to 141 nm by measuring DLS [41].
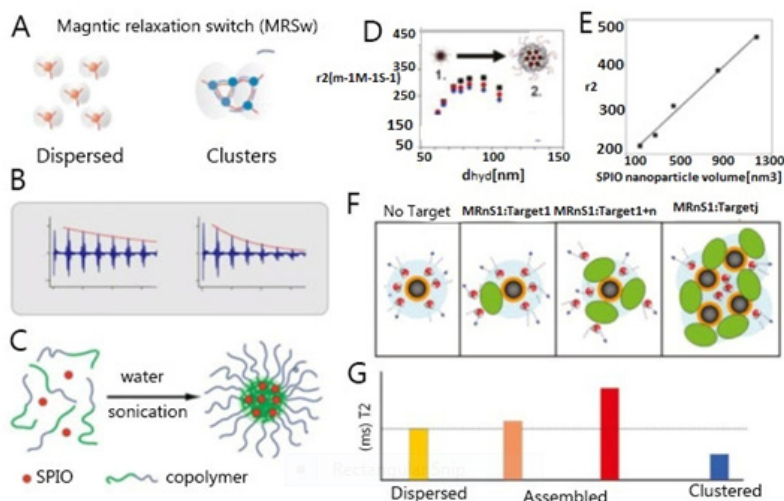

Figure 5. Assembly state and the effect on T2 relaxivity

Figure 5 (A and B) Illustration of magnetic relaxation switching (MRSw) assay and the changes in NMR signal after the aggregation of MNPs. Schematic illustration of the assembled micelle formation of MNPs. (D and E) The r_2 values of SPIO clusters as a function of the cluster size. (F and G) The assembly state-dependent aggregating architectures of MNPs in the presence of targets. The T_2 relaxation time increases in assembled structures and then decreases in clustered structures [2].

Numerous biomedical and bioengineering applications use iron oxide nanoparticles, which are members of the ferromagnetic class of magnetic materials. Maghemite (γ-Fe_2O_3), mixed ferrites (MFe_2O_4), and magnetite (Fe_3O_4) are three different forms of iron oxide-based nanoparticles. After surface modification, Superparamagnetic Iron Oxide Nanoparticles (SPION) are produced that can be used for MRI, MPI, targeted drugs, proteins, antibodies, nucleic acid delivery, hyperthermia, biosensing, tissue repair, and separation of biomolecules [23].

This extensive list of uses is brought about by SPION's magnetic characteristics as well as the fact that they may be synthesized in a variety of forms and sizes. When exposed to an external magnetic field, SPION has strong magnetic moments, and when the magnetic field is removed, there are no magnetic moments left [42,43]. Preclinical and clinical trials have examined a large number of iron oxide nanoparticles, and some of them have been commercialized. However, due to the availability of substitute diagnostic probes and protocols, some of the approved SPION have since been revoked [23].

CONCLUSION

There are numerous methods for creating iron oxide nanoparticles, each of which has benefits and drawbacks. The most widely used synthetic processes include sol-gel, microemulsion, thermal decomposition, co-precipitation, and thermal decomposition. To customize nanoparticle properties for biomedical applications, it is essential to manage critical factors such as core size, size distribution, crystallinity, shape, and saturation magnetization. Iron oxide nanoparticles' surfaces can be modified with polymers to enhance their biocompatibility, colloidal stability in challenging biological settings, and in vivo performance. Iron oxide nanoparticles are widely utilized in medicine to make diagnoses. Iron oxide nanoparticles can be utilized as T_1-weighted or T_2/T_2^*-weighted MR contrast agents depending on the size of their core. Ferumoxide and ferucarbotran have been used to visualize liver metastases and malignancies. The FDA has given Ferumoxsil approval as an oral contrast agent for gastrointestinal imaging. In clinical trials, ferumoxtran and Ferumoxytol are being used to image lymph node metastases, particularly in prostate cancer. Ferumoxytol, ferumoxtran, and feruglose have all been considered potential blood pool agents for vascular imaging, and ferumoxtran-based USPIO has been explored for imaging insulitis.

REFERENCES

1. Mudry, K.M., Plonsey, R., and Bronzino, J.D., Biomedical imaging. *CRC press*,**2003**.

2. Rosen, J.E., et al., Iron oxide nanoparticles for targeted cancer imaging and diagnostics. *Nanomedicine: Nanotechnology, Biology and Medicine*,**2012**.8(3):p. 275-290.

3. Kumar, B., et al., Synthesis of in situ immobilized iron oxide nanoparticles (Fe3O4) on microcrystalline cellulose: Ecofriendly and recyclable catalyst for Michael addition. *Applied Organometallic Chemistry*,**2022**.36(1):p. e6455.

4. Stolyar, S.V., et al., Polysaccharide-coated iron oxide nanoparticles: Synthesis, properties, surface modification. *Materials Letters*,**2021**.284(1):p. 128920.

5. Xia, L., et al., Preparation and evaluation of LA-PEG-SPION, a targeted MRI contrast agent for liver cancer. *Open Life Sciences*,**2022**.17(1):p. 952-959.

6. Antonelli, A., and Magnani, M., SPIO nanoparticles and magnetic erythrocytes as contrast agents for biomedical and diagnostic applications. *Journal of Magnetism and Magnetic Materials*,**2022**.541:p. 168520.

7. Dadfar, S.M., et al., Size-isolation of superparamagnetic iron oxide nanoparticles improves MRI, MPI and hyperthermia performance. *Journal of nanobiotechnology*,**2020**.18(1):p. 1-3.

8. Shi, X., Sun, Y., and Shen, L., Preparation and in vivo imaging of a novel potential αvβ3 targeting PET/MRI dual-modal imaging agent. *Journal of Radioanalytical and Nuclear Chemistry*,**2022**.331(9):p. 3485-3494.

9. Homeira, F. Design and Simulation of the Source (Wiggler) and Medical Beamline of Iranian Light Source Facility (ILSF) for Medical Applications. Biostat Biom Open Access J,2022. 10(4): p. 555793

10. Zhou, W., et al., Glu-Urea-Lys Scaffold Functionalized Superparamagnetic Iron Oxide Nanoparticles Targeting PSMA for In Vivo Molecular MRI of Prostate Cancer. *Pharmaceutics*,**2022**.14(10):p. 2051.

11. Rowe, S.P., and Pomper, M.G., Molecular imaging in oncology: Current impact and future directions. *CA: a cancer journal for clinicians*, **2022**.72(4):p. 333-352.

12. Gu, N., and Sheng, J., Introduction to Nanomedicine. *InNanomedicine*,**2022**:p. 1-14.

13. Zhao, Z., et al., Recent advances in engineering iron oxide nanoparticles for effective magnetic resonance imaging. *Bioactive Materials*,**2021**.

14. Wang, L., et al.,Engineering magnetic micro/nanorobots for versatile biomedical applications. *Advanced Intelligent Systems*,**2021**.3(7):p. 2000267.

15. Bronzino, J.D., and Peterson, D.R., editors. Biomedical signals, imaging, and informatics. *Taylor & Francis*,**2015**.

16. Li, M., et al., Progress in nanorobotics for advancing biomedicine. *IEEE Transactions on Biomedical Engineering*,**2020**.68(1):p. 130-147.

17. Varadan, V.K., Chen, L., and Xie, J., Nanomedicine: design and applications of magnetic nanomaterials, nanosensors and nanosys-tems. *John Wiley & Sons*,**2008**.

18. Park, C., Took, C.C., and Seong, J.K., Machine learning in biomedical engineering. *Biomedical Engineering Letters*, **2018**.8(1):p. 1-3.

19. Baccouche, H., et al., Diagnostic synergy of non-invasive cardiovascular magnetic resonance and invasive endomyocardial biopsy in troponin-positive patients without coronary artery disease. *European heart journal*,**2009**.30(23):p. 2869-2879.

20. Corek E. Superparamagnetic iron oxide nanoparticles for imaging and drug delivery (Doctoral dissertation, University_of_Basel), **2020**.

21. Li, Q., et al.,Review of spectral imaging technology in biomedical engineering: achievements and challenges. *Journal of biomedical optics*,**2013**.18(10):p. 100901.

22. Li, G., et al., Non-invasive tests of non-alcoholic fatty liver disease. *Chinese Medical Journal*,**2022**.135(05):p. 532-546.

23. Martínez-González, R., Estelrich, J., and Busquets, M.A., Liposomes loaded with hydrophobic iron oxide nanoparticles: suitable T2 contrast agents for MRI. *International Journal of Molecular Sciences*, **2016**.17(8):p. 1209.

24. Hendee, W.R., et al., The National Institute of Biomedical Imaging and Bioengineering: history, status, and potential impact. *Annals of biomedical engineering*,**2002**.30(1):p. 2-10.

25. Busch, A., et al., Metal Artefact Reduction Sequences (MARS) in Magnetic Resonance Imaging (MRI) After Total Hip Arthroplasty (THA). A Non-Invasive Approach for Preoperative Differentiation Between Periprosthetic Joint Infection (PJI) and Aseptic Complications?, **2022**.

26. Selvaraj, E.A., et al.,Diagnostic accuracy of elastography and magnetic resonance imaging in patients with NAFLD: a systematic review and meta-analysis. *Journal of hepatology*, **2021**.75(4):p. 770-785.

27. Vrenken, H., et al., Opportunities for understanding MS mechanisms and progression with MRI using large-scale data sharing and artificial intelligence. *Neurology*,**2021**.97(21):p. 989-999.

28. Miao, Y., et al., Structure–Relaxivity Mechanism of an Ultrasmall Ferrite Nanoparticle T1 MR Contrast Agent: The Impact of Dopants Controlled Crystalline Core and Surface Disordered Shell. Nano Letters,**2021**.21(2):p.1115-1123.

29. Mikhailov, A.V., et al.,Comprehensive evaluation of electrophysiological and 3D structural features of human atrial myocardium with insights on atrial fibrillation maintenance mechanisms. *Journal of molecular and cellular cardiology*, **2021**.151:p. 56-71.

30. Pallares, R.M., et al., Delineating toxicity mechanisms associated with MRI contrast enhancement through a multidimensional toxicogenomic profiling of gadolinium. *Molecular Omics*,**2022**;18(3):p. 237-248.

31. Wu, W., et al., Glioblastoma multiforme (GBM): An overview of current therapies and mechanisms of resistance. *Pharmacological Research*,**2021**.171:p. 105780.

32. Jun, Y.W., Lee, J.H., and Cheon, J., Chemical design of nanoparticle probes for high-performance magnetic resonance imaging. *Angewandte Chemie International Edition*, **2008**.47(28):p. 5122-5135.

33. Anderson, E.W., et al., Proton and pion spectra from proton-proton interactions at 10, 20, and 30 BeV/c. *Physical Review Letters*,**1967**.19(4):p.198.

34. Klem, R.D., et al., Measurement of asymmetries of inclusive pion production in proton-proton interactions at 6 and 11.8 GeV/c. *Physical Review Letters*,**1976**.36(16):p. 929.

35. Bauşic, A., et al., Transvaginal Ultrasound vs. Magnetic Resonance Imaging (MRI) Value in Endometriosis Diagnosis. *Diagnostics*,**2022**.12(7):p. 1767.

36. Schweiger, W., et al., Separable representation of the nuclear proton-proton interaction. *Physical Review C*,**1983**.27(2):p. 515.

37. Lee, N., and Hyeon, T., Designed synthesis of uniformly sized iron oxide nanoparticles for efficient magnetic resonance imaging contrast agents. *Chemical Society Reviews*, **2012**.41(7):p. 2575-2589.

38. CHANG, C.A., Magnetic resonance imaging contrast agents design and physicochemical properties of gadodiamide. *Investigative radiology*,1993.28:p. S21-AS27.

39. Menze, B., et al., Analyzing magnetic resonance imaging data from glioma patients using deep learning. *Computerized medical imaging and graphics*,**2021**.88:p. 101828.

40. Huang, P., and Zhang, M., Magnetic Resonance Imaging Studies of Neurodegenerative Disease: From Methods to Translational Research. *Neuroscience Bulletin*,**2022**:p. 1-4.

41. Fadeyev, F.A., et al., Biological Impact of γ-Fe2O3 Magnetic Nanoparticles Obtained by Laser Target Evaporation: Focus on Magnetic Biosensor Applications. *Biosensors*,**2022**.12(8):p. 627.

42. Jasim, K., Tumor-Targeted Conjugated Polymer Nanoparticles with Encapsulated Iron and Its Biomedical Application for In Vitro Killing of Melanoma Cell Lines Through Ferroptosis Assisted Chemodynamic Therapy (CDT),**2019**.

43. Humphreys, K., et al., Medical applications of terahertz imaging: a review of current technology and potential applications in biomedical engineering. *InThe 26th Annual International Conference of the IEEE Engineering in Medicine and Biology Society*, **2004**.1: p. 1302-1305.